

# Bounding Localization Errors with Student Distribution for Road Vehicles

Joelle Al Hage, Philippe Xu and Philippe Bonnifait \*

## 1 Introduction

Localization integrity was initially developed for aeronautical applications in order to provide a measure of confidence for GNSS based navigation solutions. It is associated with a target integrity risk which represents the maximum allowed probability that the error in position exceeds a given limit without warning the user. This limit is known as the Protection Level (PL). Recently, the integrity concept became of interest for non-aeronautical navigation. Indeed, the GNSS integrity for land vehicles was firstly introduced for liability-critical applications such as Electronic Toll Collection (ETC) and *pay as you drive* insurance [1]. The purpose is to avoid wrong decision (e.g. wrong tolls invoice,...). Moreover, the integrity concept is vital for autonomous vehicles where a PL should be generated in order to increase the system safety.

Aeronautical integrity methods can not be applied directly to road vehicles applications for different reasons. Indeed, classical GNSS integrity methods are affected by various limitations in these contexts:

- The approaches based on the Fault Detection and Exclusion (FDE) assume often one fault at a time which cannot be verified in road applications since the main error sources in such environments are multipath and NLOS [2][3],
- The assumption of zero mean Gaussian distribution cannot be verified in these environments because of biases errors due to multipath and NLOS [4][5],
- The requirements of integrity in aviation operations could be too conservative for vehicular applications which increase the system unavailability [6],
- The classical methods of computation of PL do not take into account the presence of other sensors like the IMU, camera, LiDAR or map.

The integrity monitoring methods can be classified into measurement rejection approach (known also as Fault Detection and Exclusion (FDE)) and error characterization approach [1], [7]. The two approaches lead to different protection level sizes

---

\*The authors are with Heudiasyc, UMR 7253, Université de Technologie de Compiègne, Sorbonne Universités, 57 Avenue de Landshut, 60200 Compiègne, France. The authors are also members of the SIVALab, a shared laboratory between Renault/Heudiasyc/CNRS/UTC.

and therefore different availability. Indeed, FDE approaches may fail to give a navigation solution with an associated protection level. However, the error characterization approaches lead to a large protection in presence of faulty measurements which may increase the unavailability of the system.

## 2 Proposed approach for road vehicles

In this paper, the approach that we propose is divided into two separate parts:

- Position estimation after a fault detection and exclusion step. The informational form of the Kalman Filter is used for the estimation [8].
- Error modeling after removing all detected faulty measurements from the system in order to compute a protection level. For this part, we aim to avoid an underestimation of the PL that may be due to an underestimation of the covariance matrix of the filter or from non Gaussian error distributions. The latter may result from the linearization of nonlinear models or from outliers that remain in the data after the FDE stage. Therefore, when computing the PL, we propose to replace the multivariate Gaussian distribution by a multivariate student distribution which is heavy tailed and hence permits to cope with errors not taken into account when using the Gaussian distribution [9].

An overview of the method is given in figure 1.

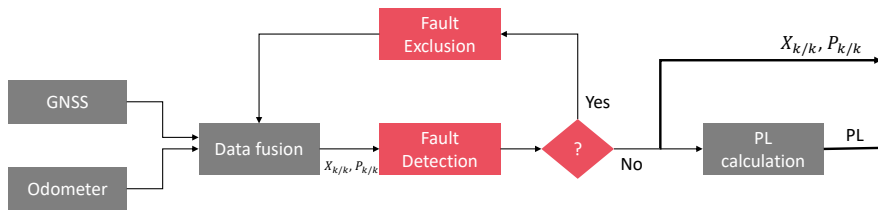


Figure 1: Architecture of the proposed method. GNSS and odometer data are combined in a FDE loop. The PL is computed from the estimated position and covariance matrix when no more faults are detected.

### 2.1 Protection Level for road vehicle

The informational form of the error propagation at epoch  $k$  can be expressed as:

$$e_{y,k} = e_{y,k/k-1} + \sum_{i=1}^n H_{i,k}^T R_{i,k}^{-1} e_{Z,i,k} \quad (1)$$

$$= Y_{k/k-1} e_{X,k/k-1} + \sum_{i=1}^n H_{i,k}^T R_{i,k}^{-1} e_{Z,i,k} \quad (2)$$

$$= Y_{k/k-1} F_k e_{X,k-1} + \sum_{i=1}^n H_{i,k}^T R_{i,k}^{-1} e_{Z,i,k} \quad (3)$$

where:

$Y_k$  and  $e_{y,k}$  represent respectively the information matrix and the informational form of the error propagation  $e_{X,k}$ :

$$Y_k = P_k^{-1} \quad (4)$$

$$e_{y,k} = Y_k e_{X,k} \quad (5)$$

$P_k$  is the covariance matrix,

$e_{Z,i,k}$  is the error of measurement  $Z_i$  at epoch  $k$ .

The error propagation can be written as

$$e_{X,k} = \underbrace{Y_{k/k}^{-1} Y_{k/k-1} F_k e_{X,k-1}}_{\sim N_p(0, R_p)} + Y_{k/k}^{-1} \sum_{i=1}^n H_{i,k}^T R_{i,k}^{-1} e_{Z,i,k} \quad (6)$$

$$Y_{k/k}^{-1} H_{i,k}^T R_{i,k}^{-1} e_{Z,i,k} \sim N(0, R_{Z,i,k})$$

$e_{X,k-1}$  is the projection to the state model of the errors measurement accumulated at the previous epoch,

$H_{i,k}$  is the observation matrix associated to the observation type  $Z_i$  (it is a Jacobian for a non linear model),

$R_{i,k}$  is the covariance associated to the observation noise  $Z_i$ ,

$F_k$  is the state transition matrix (it is a Jacobian for a non linear model),

$n$  number of observations.

If the position error  $e_{X,k}$  is distributed according to a zero-mean multivariate Gaussian distribution then:  $e_{X,k} \sim N(0, C_k)$ ,

$C_k$  is the covariance matrix computed as

$$C_k = R_{p,k} + \sum_{i=1}^n R_{Z,i,k} \quad (7)$$

$R_{p,k}$  and  $R_{z,i,k}$  are obtained from linear operation on  $Y_{k/k}^{-1}Y_{k/k-1}F_k e_{X,k-1}$  and  $Y_{k/k}^{-1}H_{i,k}^T R_{i,k}^{-1} e_{Z,i,k}$  respectively:

$$R_{p,k} = Y_{k/k}^{-1}Y_{k/k-1}F_k R_{p,k-1} F_k^T Y_{k/k-1} Y_{k/k}^{-1} \quad (8)$$

$$R_{z,i,k} = Y_{k/k}^{-1}H_{i,k}^T R_{i,k}^{-1} H_{i,k} Y_{k/k}^{-1} \quad (9)$$

Once the covariance of the error is calculated (equation 7), the objective is to obtain a consistent protection level. For this purpose,  $C$  will be considered as the covariance matrix of a multivariate student distribution with a fixed degree of freedom  $N$ . Notice that when  $N \rightarrow \infty$ , the student distribution converges to a Gaussian distribution.

The protection level is expressed as:

$$PL_k(\alpha) = K(\alpha, N) \max(\text{eigenvalue}(C_k)) \quad (10)$$

where  $K$  is obtained from a multivariate t-distribution with degree of freedom  $N$  and covariance matrix  $C$  according to a given confidence level  $\alpha$ . By integrating the density function of the multivariate t-distribution using the norm of the error between the protection level and infinite,  $K(\alpha, N)$  can be computed by solving numerically equation 11 [10]:

$$\alpha = \frac{2}{B(\frac{d}{2}, \frac{N}{2})} \int_K^{\infty} \frac{y^{d-1}}{(1+y^2)^{\frac{N+d}{2}}} dy \quad (11)$$

A modification of equation 10 can be done by replacing  $C_k$  by the covariance matrix  $P_{k/k}$  of the navigation filter. The way  $K(\alpha, N)$  is computed remains unchanged and one gets another expression:

$$PL_k(\alpha) = K(\alpha, N) \max(\text{eigenvalue}(P_{k/k})) \quad (12)$$

A comparison between the two approaches will be given in section 4.

### 3 Application to loosely coupled GNSS/odometer

At instant  $k$  the state vector is considered to be the position and the heading of the vehicle:

$$X = [ x \quad y \quad \theta ]^T \quad (13)$$

The propagation equation is given by

$$X_{k+1/k} = X_{k/k} + A_k u_k + \alpha_k \quad (14)$$

$$= f(X_{k/k}, u_k) + \alpha_k \quad (15)$$

where

$$A_k = \begin{pmatrix} \cos(\theta_{k/k} + \frac{\omega_k}{2}) & 0 \\ \sin(\theta_{k/k} + \frac{\omega_k}{2}) & 0 \\ 0 & 1 \end{pmatrix} \quad (16)$$

$u_k$  is the input vector, it consists of the elementary displacement and rotation of the vehicle:  $u_k = [\Delta_k, \omega_k]$

$$\Delta_k = \frac{r_r \Delta q_{r,k} + r_l \Delta q_{l,k}}{2}$$

$r_r$  and  $r_l$  represents respectively the radius of the right and left wheel.

$\Delta q_{r,k}$  and  $\Delta q_{l,k}$  correspond to the elementary rotations of the right and left wheels respectively.

$\omega_k$  is obtained from the gyro.

The covariance matrix is computed as:

$$P_{k+1/k} = F_k P_{k/k} F_k^T + B_k (Q_u)_k B_k^T + Q_k \quad (17)$$

where:

$Q_u$  is the covariance matrix associated to the input vector  $u_k$

$F_k$  and  $B_k$  are Jacobian matrices;  $F_k = \frac{\partial f}{\partial x} |_{X=X_{k/k}}$  and  $B_k = \frac{\partial f}{\partial u} |_{u=u_k}$

$Q_k$  is the covariance associated to the process noise  $\alpha_k$  modeled as Gaussian white noise.

The information matrix and information vector are obtained respectively as

$$Y_{k+1/k} = P_{k+1/k}^{-1} \quad (18)$$

$$y_{k+1/k} = Y_{k+1/k} X_{k+1/k} \quad (19)$$

The fusion of the dead-reckoning measurements with the GNSS measurements is done through a loosely coupled architecture. The observation model is expressed as in equation 20:

$$Z_1 = \begin{pmatrix} x_{GNSS} \\ y_{GNSS} \end{pmatrix} \quad (20)$$

$$x_{GNSS} = t_x \cos \theta - t_y \sin \theta + x \quad (21)$$

$$y_{GNSS} = t_x \sin \theta + t_y \cos \theta + y \quad (22)$$

where  $t_x$  and  $t_y$  are the translation of the antenna with respect to the body frame (lever of arm of the antenna).

The observation matrix is given by:

$$H_1 = \begin{pmatrix} 1 & 0 & -t_x \sin \theta_{k/k-1} - t_y \cos \theta_{k/k-1} \\ 0 & 1 & t_x \cos \theta_{k/k-1} - t_y \sin \theta_{k/k-1} \end{pmatrix} \quad (23)$$

The information matrix and information vector are updated as

$$Y_{k/k} = Y_{k/k-1} + I_k \quad (24)$$

$$y_{k/k} = y_{k/k-1} + i_k \quad (25)$$

with:

$$I_k = H_{1,k} R_{1,k}^{-1} H_{1,k} \quad (26)$$

$$i_k = H_{1,k} R_{1,k}^{-1} [(Z_{1,k} - \hat{Z}_1) + H_{1,k} X_{k/k-1}] \quad (27)$$

## 4 Preliminaries experimental results

The GNSS receiver used in this experimentation is a Ublox 8T which is a multi constellation (GPS/GLONASS) GNSS receiver. We report in this section an experiment carried out in a constrained environment which particularly biases the GNSS fixes. Figure 2 shows the estimated trajectory compared to the ground truth. A bias up to 6 meters is clearly visible. The estimated standard deviations provided by the GNSS receiver are in the order of one meter which is inconsistent with the observed errors.

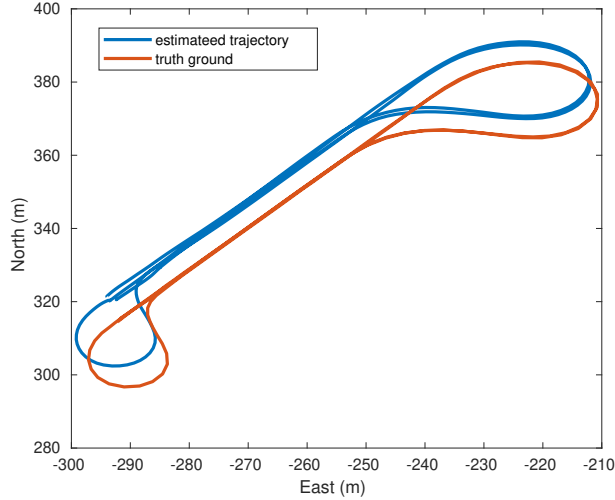


Figure 2: Trajectory estimation (blue) compared to the ground truth (red)

We give here some results (which will be more deeply explain in the final version of the paper) on the performance of the protection level as given in equations 10 and 12.

Figure 3 shows the position error and the protection level corresponding to a target integrity risk  $\alpha=10^{-4}$  and a degree of freedom  $N = 2.1$ . It can be seen, that a PL with entry  $P_{k/k}$  is more conservative than the one with entry  $C_k$ .

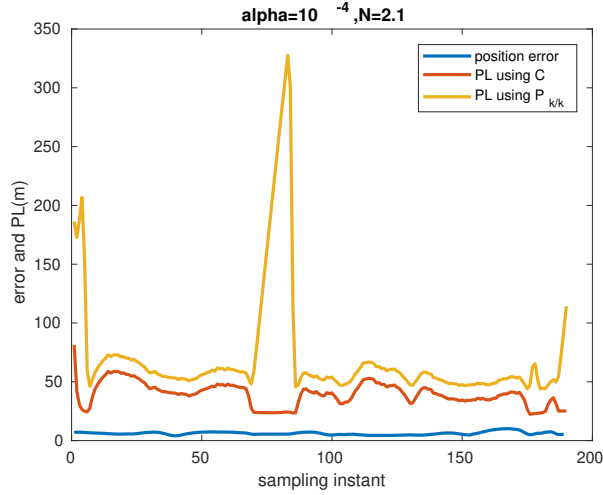


Figure 3: Error and PLs for a degree of freedom  $N = 2.1$  and  $\alpha = 10^{-4}$

Figure 4 and 5 show the protection levels for a degree of freedom  $N = 3$  and  $N = 4$  respectively. The consistency of the protection level decreases when the number of degree of freedom increases, so when the distribution approaches a Gaussian.

Tables 1 shows the inconsistency rate (rate of  $PL < error$ ) for a covariance matrix equal to  $C_k$  and  $P_{k/k}$ , and for different values of the degree of freedom. The target integrity risk was fixed to  $10^{-4}$ . The error inconsistency rate is 0 for a multivariate t-distribution with degree of freedom less than 3 and increases with the number of degree of freedom. The method that use  $P_{k/k}$  is more consistent than the one that uses  $C_k$  when the degree of freedom increases. Table 2 shows the same results but with a higher target integrity risk ( $\alpha = 10^{-3}$ ). The error rate null for  $N = 2.1$ , begins to increase for a degree of freedom higher than 2.5. It can be noted that in this test, almost the same results are obtained for  $(N = 4, \alpha = 10^{-4})$  and  $(N = 3, \alpha = 10^{-3})$ .

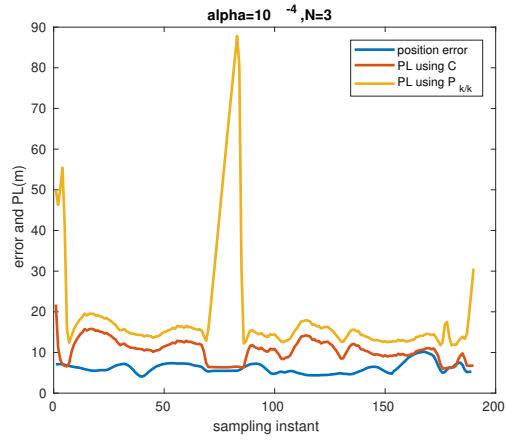


Figure 4: Error and PLs for a degree of freedom  $N = 3$  and  $\alpha = 10^{-4}$

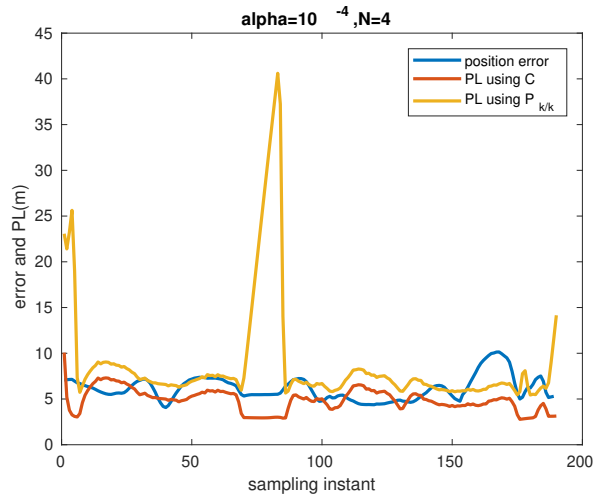


Figure 5: Error and PLs for a degree of freedom  $N = 4$  and  $\alpha = 10^{-4}$

N	inconsistency rate with $C_k$	inconsistency rate with $P_{k/k}$
2.1	0	0
2.5	0	0
2.7	0	0
3	0.0476	0
4	0.7302	0.2593
100	0.9947	0.8995

Table 1: Inconsistency rate for  $\alpha = 10^{-4}$



N	inconsistency rate with $C_k$	inconsistency rate with $P_{k/k}$
2.1	0	0
2.5	0.2593	0.0053
2.7	0.4656	0.0794
3	0.7302	0.2593
4	0.9947	0.8730
100	0.9947	0.9048

Table 2: Inconsistency rate for  $\alpha = 10^{-3}$

## 5 Outlook

In the paper, we propose a new method of protection level calculation adapted to road vehicles. The idea is to replace when computing PL the multivariate Gaussian distribution by a multivariate student distribution which is heavy tailed. The approach computes a protection level after removing the main faulty data from the system.

The first results obtained with a Ublox receiver show that the computation of a PL is consistent with a Student distribution (whereas it would be too optimistic with a Gaussian assumption) in road environments where GNSS estimates can be significantly biased. A Student distribution with a degree of freedom less than 3 under a target integrity risk of  $10^{-4}$  is more consistent for the protection level calculation in this kind of environment. Likewise, a comparison between two methods proposed to determine the covariance matrix is handled.

In the final version of the paper, we will explain in details the stages of the method that we propose and we will report more experimental results.

## References

- [1] J. Cosmen-Schortmann, M. Azaola-Saenz, M. A. Martinez-Olague, and M. Toledo-Lopez, “Integrity in urban and road environments and its use in liability critical applications”, in *Position, Location and Navigation Symposium, 2008 IEEE/ION*, IEEE, 2008, pp. 972–983.
- [2] M. S. Braasch, “Multipath effects”, *Global Positioning System: Theory and Applications.*, vol. 1, pp. 547–568, 1996.
- [3] P. D. Groves, Z. Jiang, L. Wang, and M. K. Ziebart, “Intelligent urban positioning using multi-constellation GNSS with 3d mapping and NLOS signal detection”, in *Proceedings of the 25th International Technical Meeting of The Satellite Division of the Institute of Navigation (ION GNSS 2012)*, 2012, pp. 458–472.
- [4] K. Ali, M. Pini, and F. Dovis, “Measured performance of the application of EGNOS in the road traffic sector”, *GPS solutions*, vol. 16, no. 2, pp. 135–145, 2012.

- [5] J. Marais, M. Berbineau, and M. Heddebaut, “Land mobile GNSS availability and multipath evaluation tool”, *IEEE transactions on vehicular technology*, vol. 54, no. 5, pp. 1697–1704, 2005.
- [6] D. Salos, A. Martineau, C. Macabiau, B. Bonhoure, and D. Kubrak, “Receiver autonomous integrity monitoring of GNSS signals for electronic toll collection”, *IEEE transactions on intelligent transportation systems*, vol. 15, no. 1, pp. 94–103, 2014.
- [7] M. Worner, F. Schuster, F. Dolitzscher, C. G. Keller, M. Haueis, and K. Dietmayer, “Integrity for autonomous driving: A survey”, in *Position, Location and Navigation Symposium (PLANS), 2016 IEEE/ION*, IEEE, 2016, pp. 666–671.
- [8] C. Zhang and H. Wang, “Decentralized multi-sensor data fusion algorithm using information filter”, in *2010 International Conference on Measuring Technology and Mechatronics Automation*, vol. 1, Mar. 2010, pp. 890–893.
- [9] A. Dhital, J. B. Bancroft, and G. Lachapelle, “A new approach for improving reliability of personal navigation devices under harsh gnss signal conditions”, *Sensors*, vol. 13, no. 11, pp. 15 221–15 241, 2013.
- [10] P. F. Navarro Madrid, “Device and method for computing an error bound of a kalman filter based gnss position solution”, 20 160 109 579, Apr. 2016.